Lithium- and Proton-Driven Redox Reactions in BIMEVOX-Type Phases

Sébastien Patoux,[†] Rose-Noëlle Vannier,[‡] Gaëtan Mairesse,*[,‡] Guy Nowogrocki,[‡] and Jean-Marie Tarascon*[,†]

Laboratoire de Réactivité et de Chimie des Solides, UPRES-A 6007, Université de Picardie Jules Verne, 33 rue Saint-Leu, 80039 Amiens Cedex, France, and Laboratoire de Cristallochimie et Physicochimie du Solide, UPRES-A 8012, Ecole Nationale Supèrieure de Chimie de Lille, B.P. 108, 59652 Villeneuve d'Ascq Cedex, France

Received July 31, 2000. Revised Manuscript Received October 30, 2000

$Bi_4V_2O_{11}$ reduction was followed using two methods: high-temperature X-ray diffraction under H_2 flow and oxygen removal with Zr acting as an oxygen acceptor. In both cases, the reversible domain of reduction of $Bi_4V_2O_{11}$ appeared to be limited to one-third of V^V and therefore to the formation of a $Bi_6V_3O_{16}$ ($Bi_4V_2O_{10.66}$) phase. Various BIMEVOX/electrolyte/Li cells were characterized evidencing the progressive reduction of the BIMEVOX materials. Pursuing the cell discharge down to 0.02 V resulted in a full amorphization of the material together with an uptake of 32 lithium ions per formula unit. From both electrochemical and in situ X-ray diffraction data extended to the BIMEVOX (ME = Bi, Ta), a two-step mechanism is proposed involving first an oxygen removal concomitant with the formation of Li_2O and the $Bi_6V_3O_{16}$ ($Bi_4V_2O_{10.66}$) phase, followed by a Li-driven decomposition of the latter in an inert Li_2O matrix, a Li-alloying Bi phase and a vanadate.

Introduction

Oxide anion conductors such as yttria-stabilized zircona (YSZ) have long been studied as solid-oxide electrolytes in various applications ranging from oxygen sensors and electrochemical oxygen pumps to high-temperature solid oxide fuel cells (SOFC). Such a panel of applications has prompted the search for better solid-oxide conductors and the discovery of new classes of materials, such as lanthanum-doped gallates[1] or rare-earth Bi-oxides,[2] of potential interest for oxygen conduction. In this field, the so-called BIMEVOX family displays the best properties at moderate temperatures (300−500 °C). This family of materials derives from $Bi_4V_2O_{11}$ by partial substitution for vanadium with a variety of metals (ME).[3]

Depending on the temperature, the parent $Bi_4V_2O_{11}$ compound exhibits three polymorphs, denoted α, β, and γ, with α being stable from room temperature up to 430 °C, β between 430 and 570 °C, and γ at 570 and above. The high-temperature form is the most disordered and thereby the most interesting for its conducting properties, the σ value being $> 10^{-1}$ S cm^{-1} at $T > 500$ °C. Such a high oxygen conduction is due to the bidimensional character of its structure based on highly covalent $[Bi_2O_2]^{2+}$ layers sandwiched between highly disordered oxygen deficient perovskite $[VO_{3.5}\square_{0.5}]^{2-}$ slabs characterizing an intrinsic anionic conductor (Figure 1).[4] Once the importance of the γ-phase was elucidated, its range of stability was lowered down to lower temperatures by means of chemical substitutions, hence the appearance of the BIMEVOX family.[5] Due to their low stability under a reducing atmosphere, these materials cannot be used directly in SOFC but are developed as membrane for oxygen generators.

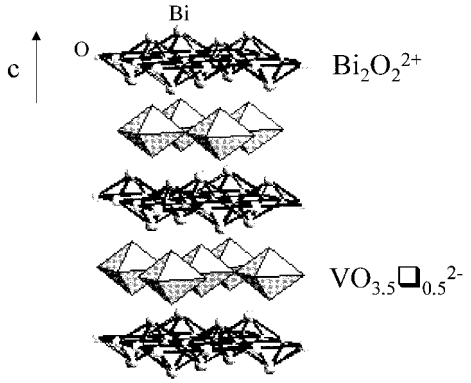

Figure 1. $Bi_4V_2O_{11}$ idealized crystal structure.

Under a hydrogen atmosphere, the parent compound, $Bi_4V_2O_{11}$, undergoes a $V^V \rightarrow V^{IV}$ reduction leading to the formation of the $Bi_6V_3O_{16}$ ($Bi_4V_2O_{10.66}$) phase having one V^{IV} for two V^V before ultimate destruction into Bi and V_2O_3. This mixed valence V^V-V^{IV} phase was initially evidenced by Joubert et al.,[6] who refined its crystal structure in the *Pnma* space group with $a = 5.47$, $b = 17.25$, and $c = 14.92$ Å parameters. This oxygen-

[†] Université de Picardie Jules Verne.
[‡] Ecole Nationale Supèrieure de Chimie de Lille.

(1) Ishihara, T.; Matsuda, H.; Takita, Y. *J. Am. Chem. Soc.* **1994**, *116*, 3801.
(2) Boivin, J. C.; Mairesse, G. *Chem. Mater.* **1998**, *10*, 2870.
(3) Lazure, S.; Vernochet, C.; Vannier, R. N.; Nowogrocki, G.; Mairesse, G. *Solid State Ionics* **1996**, *90*, 117.
(4) Mairesse, G. *C. R. Acad. Sci. Paris* **1999**, *t.2* (série IIc), 651.
(5) Abraham, F.; Boivin, J. C.; Mairesse, G.; Nowogrocki, G. *Solid State Ionics* **1990**, *40/41*, 934.
(6) Joubert, O.; Jouanneaux, A.; Ganne, M. *Nucl. Instrum. Methods Phys. Res.* **1995**, *B97*, 119.

10.1021/cm001149c CCC: $20.00
Published on Web 01/26/2001

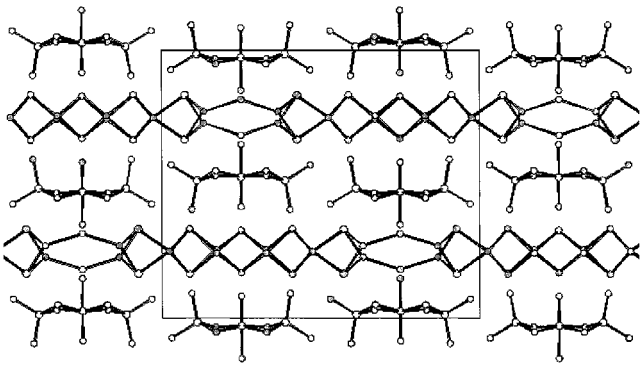

Figure 2. [100] projection of $Bi_6V_3O_{16}$ ($Bi_4V_2O_{10.66}$) crystal structure.

deficient phase that exhibits a 3-fold superstructure along the *b*-axis can simply be viewed as an Aurivillius bronze built up with $[Bi_6O_6]^{6+}$ layers sandwiched between two $[V_3O_{10}]^{6-}$ ribbons (Figure 2). This structure was confirmed by Huvé et al. by TEM and HREM studies.[7] However Galy et al.[8] claimed the existence of a $(Bi_2O_2)_2(V^V_{1-x}V^{IV}_x)_2O_{7-x}$ solid solution for x values within the entire range $0 \leq x \leq 1$, and therefore doubt remains about the reduction steps in $Bi_4V_2O_{11}$.

Recently a Spanish group[9] considered the possibility of using $Bi_4V_2O_{11}$ as an electrode in a lithium battery: for a Li/electrolyte/$Bi_4V_2O_{11}$ cell, up to 28 lithiums could be inserted into the positive. They characterized their lithiated materials using X-ray diffraction.[10] A contraction of the unit cell along the [0 0 1] direction was observed, and they attributed it to a "strong electrostatic interaction between lithium ions and bismuth inert pair", assuming lithium insertion. However, depending on the lithium content, no evolution of the Bragg peaks was evidenced, and only a loss of crystallinity was noticed.

Thus, does lithium insertion in the material really occur? How can the amount of inserted lithium be explained?

As an attempt to address these issues, various BIMEVOX/electrolyte/Li electrochemical cells were assembled and characterized. The parent compound, $Bi_4V_2O_{11}$, was first considered, and then experiments on BIMEVOX materials were undertaken. Since the vanadium sites in $Bi_4V_2O_{11}$ can be substituted for numerous metals including bismuth itself, a BIBIVOX.02 ($Bi_2V_{0.98}Bi_{0.02}O_{5.5-\delta}$) and a BITAVOX.15 ($Bi_2V_{0.85}Ta_{0.15}O_{5.5}$) sample that involves no change in the oxygen stoichiometry were selected.

Insertion of lithium in the structure of these materials, assuming the existence of empty sites within the oxide structure, would probably induce a V^V/V^{IV} reduction process. Therefore, prior to the electrochemical characterization, the behavior of these materials under reducing atmosphere was followed using in situ high-temperature X-ray diffraction. Then, to determine the steps of $Bi_4V_2O_{11}$ reduction, quantitative removals of oxygen from $Bi_4V_2O_{11}$ by an oxygen acceptor (Zr) in a sealed Pyrex tube were performed.

For reasons of clarity, the paper will be presented as follows. The Experimental Section will be followed by sections regarding first the chemical reduction of these materials by H_2 and Zr and then by the electrochemical approach.

Experimental Section

The starting BIMEVOX (ME = Bi, Ta) powders used in the present study were homemade by the classical ceramic method consisting in thoroughly mixing stoichiometric amounts of Bi_2O_3 (Riedel de Haën, 99.5% in purity, previously decarbonated at 600 °C for 6 h), V_2O_5 (Aldrich, 99.9%) and Ta_2O_5 (Aldrich, 99.99%). The mixed powders were placed in gold foil boats, annealed for 12 h at 600, 700, and 800 °C successively with intermediate grinding, and cooled from 800 °C to room temperature.

The samples were characterized for phase purity by means of a Guinier−De Wolf focusing camera using Cu Kα radiation. Elemental compositions were confirmed by energy dispersive spectroscopy (EDS) on a Link−Isis analyzer (ATW 6650 detector) attached to the microscope.

Room-temperature X-ray diffraction experiments were performed on a PW1710 Phillips diffractometer, using a Cu anticathode.

High-temperature X-ray diffraction was carried out on a Siemens D5000 diffractometer, Cu Kα radiation, equipped with a HTK1200 Anton Paar device and a PSD detector. The samples were heated under air atmosphere from room temperature up to 350 °C with a 0.2 °C/s rate; the atmosphere was then purged of oxygen with nitrogen for about 45 min before the sample was studied under H_2/N_2 (2.5 L/h, 2.5 L/h, 1 atm) flow. A diagram was recorded every 15 min in the 10−70° 2θ domain, with a 5 min delay before each measurement, a step of 0.0146° and a counting time of 0.15 s (i.e., a diagram was recorded in about 10 min).

Swagelok-type cell configurations were used for electrochemical testing. Lithium/BIMEVOX electrochemical cells were assembled from 1 cm^2 disks of Li foil as the negative electrode member, a Whatman GF/D borosilicate glass fiber sheet saturated with a 1 M $LiPF_6$ electrolyte solution in 1:1 (weight ratio) of dimethyl carbonate/ethylene carbonate as the separator member, and an acetone-cast plastic film as the positive electrode. This film containing 56 parts of finely divided BIMEVOX, 6 parts of super P carbon black (SP, MMM Carbon, Belgium), and 23 parts of dibutyl phthalate (DBP) dispersed in 15 parts of (poly) vinylidene-hexafluoropropylene (PVdF−HFP) (Kynar FLEX, Elf Atochem NA) was made as described elsewhere.[11] The electrochemical tests were carried out using a "Mac-Pile" automatic cycling/data recording system (Biologic SA, Claix, France) operating in galvanostatic or potentiostatic mode. In the former, the lithium composition in the "Li_xBIMEVOX" material was calculated from the elapsed time and the amount of current. Data were logged out whenever the cell voltage changed by more than 0.02 V.

Electrochemically active driven structural changes were followed by means of an in situ electrochemical cell similar to that previously described elsewhere[12] and having the cathode material directly deposited on the beryllium window, which acts as the positive current collector. Once assembled, the cell is then mounted on a SCINTAG diffractometer operating in the Bragg−Brentano geometry, having Cu Kα radiation, and connected to a Mac-Pile system for in situ testing. The battery is usually discharged and charged at very low current rates (e.g., =C/50, which means 1 Li per formula in 50 h) in order to be close to equilibrium conditions.

(7) Huvé, M.; Vannier, R. N.; Nowogrocki, G.; Mairesse, G.; Van Tendeloo, G. *J. Mater. Chem.* **1996**, *6* (8), 1339.
(8) Galy, J.; Enjalbert, R.; Millan, P.; Castro, A. *C. R. Acad. Sci. Paris* **1993**, *série II*, 43.
(9) Arroyo y de Dompablo, M. E.; Garcia-Alvarado, F.; Moran, E. *Solid State Ionics* **1996**, *91*, 273.
(10) Arroyo y de Dompablo, M. E.; Garcia-Alvarado, F.; Moran, E.; Prieto, C.; Fuess, H. *Mol. Cryst. Liq. Cryst.* **1998**, *311*, 31.
(11) Tarascon, J.-M.; Gozdz, A. S.; Schmutz C. Warren, P. C. *Solid State Ionics* **1996**, *86*, 49.
(12) Amatucci, G. G.; Tarascon, J.-M.; Klein, L. C. *J. Electrochem. Soc.* **1996**, *143*, 3.

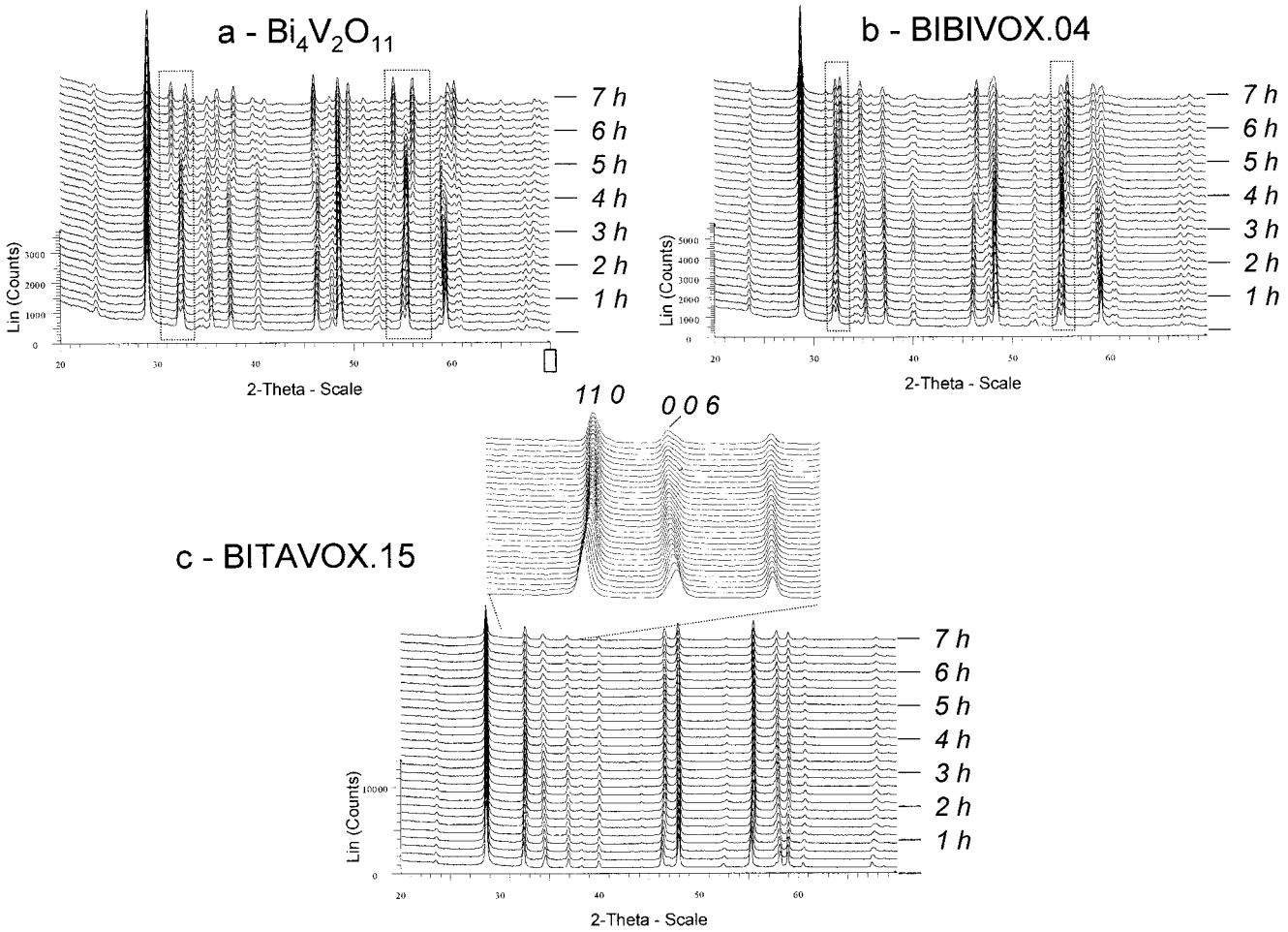

Figure 3. HTXRD at 350 °C under H_2/N_2 atmosphere corresponding to (a) $Bi_4V_2O_{11}$, (b) BIBIVOX.04, and (c) BITAVOX.15. The dotted outlined rectangles highlight the two domains in which a progressive merger of characteristic *hkl*/*khl* doublets is observed.

Results

(1) High-Temperature X-ray Diffraction under a Reducing Atmosphere. The diagrams corresponding to $Bi_4V_2O_{11}$, BIBIVOX.04 ($Bi_2V_{0.96}Bi_{0.04}O_{5.5-\delta}$), and BITAVOX.15 ($Bi_2V_{0.85}Ta_{0.15}O_{5.5}$), performed at 350 °C under a H_2/N_2 atmosphere, are reported in Figure 3.*(a) BIBIVOX Materials ($Bi_4V_2O_{11}$ (BIBIVOX.00) BIBIVOX.02 and BIBIVOX.04).* In the $Bi_4V_2O_{11}$ case, at the beginning of the reduction process, a progressive merger of the characteristic (*hkl*)/(*khl*) doublets characterizing the orthorhombic symmetry is observed giving rise to a tetragonal polymorph after about 3 hours and 30 minutes. At that time, a new phase identified as α-$Bi_6V_3O_{16}$ (or $Bi_4V_2O_{10.66}$) begins to grow, to the expense of the tetragonal ($Bi_6V_3O_{16}$) phase. Then, α-$Bi_6V_3O_{16}$ progressively and nonreversibly reduces into Bi and V_2O_3, if the reduction is further pursued. This process was described in detail elsewhere[7] and was interpreted as first the progressive formation of the $Bi_2V^{V}_{1-x}V^{IV}_{x}O_z$ solid solution with *x* increasing up to 0.33, leading to a γ-type tetragonal BIMEVOX with a random V^{V}/V^{IV} distribution. At this reduction level, a disorder−order phase transition occurs, generating the typical $[V_3O_{10}]^{6-}$ ribbons with one $V^{IV}O_6$ octahedron connected to two $V^{V}O_4$ tetrahedra (Figure 2) characterizing the α-$Bi_6V_3O_{16}$ compound.

For the first time, we investigated the reoxidation of $Bi_6V_3O_{16}$ in air and found that it occurs at 300 °C. In addition, the reactivity of $Bi_4V_2O_{11}$ in N_2 ambient (e.g., 10^{-6} atm of residual partial oxygen pressure) was studied as a function of temperature and two transformations are evidenced, the first one with the occurrence of an orthorhombic intermediate phase at 425 °C, and the second one giving rise to a tetragonal phase above 500 °C. However, when the sample is cooled to room temperature, it is partially reoxidized in a $BiV^{IV}VOX$ phase (Figure 4a). Then to follow the thermal evolution of this phase as a function of the temperature, a HTXRD experiment was performed under a N_2 flow containing traces of H_2 to prevent any reoxidation by oxygen traces (Figure 4b). The α-$Bi_6V_3O_{16}$ transformation into a β form at 400 °C and then to a γ form at 580 °C was confirmed. These transformations are reversible. On cooling, the γ → β transformation is observed at 540 °C and that of β → α occurs at 360 °C.

In a similar way, the orthorhombic BIBIVOX.02 and BIBIVOX.04 phases were studied. As BIBIVOX.02 behavior was very similar to that of $Bi_4V_2O_{11}$, only BIBIVOX.04 is reported (Figure 3b). First, it progressively transforms into a tetragonal form during the first 3 h, and then progressively gives rise to a new orthorhombic phase. When this phase was cooled to room temperature, the diffractogram of this latter is close to that of α-$Bi_6V_3O_{16}$; the orthorhombic phase observed at 350 °C corresponds to the intermediate β-$Bi_6V_3O_{16}$ polymorph. The small Bi over stoichiometry, with 0.04

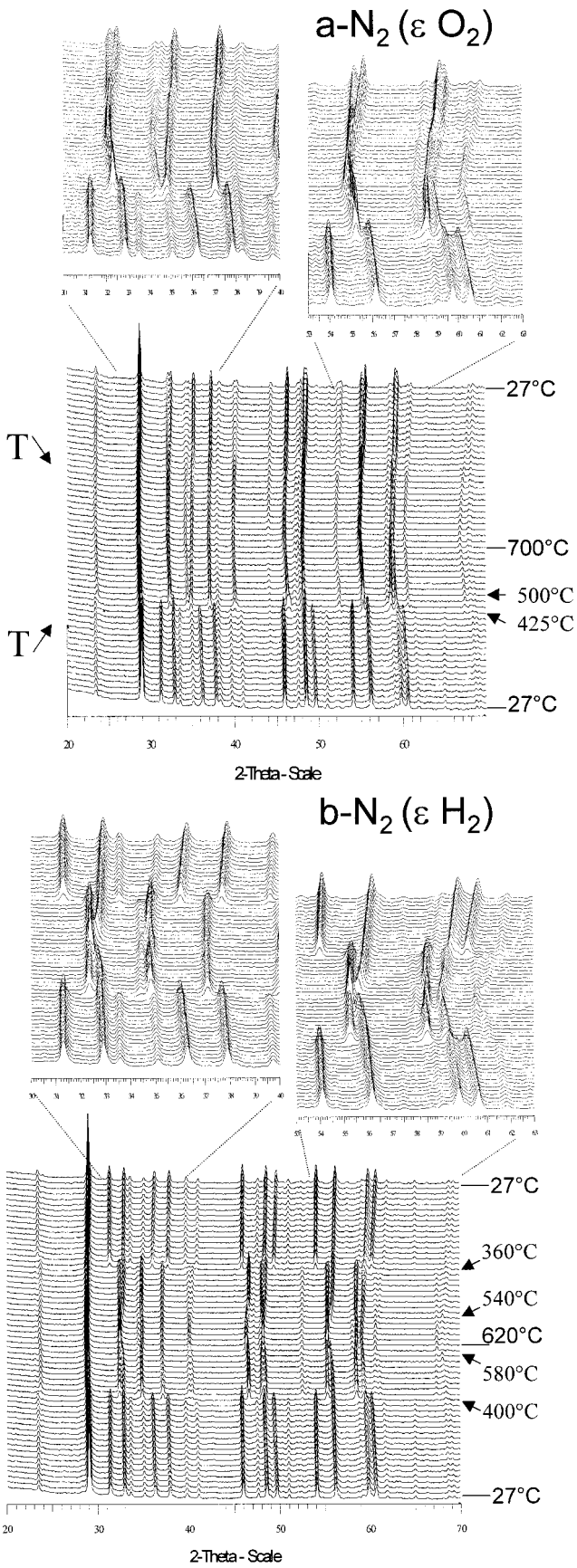

Figure 4. $Bi_6V_3O_{16}$ HTXRD from room temperature to 700 °C under (a) a N_2 atmosphere (a diffractogram was recorded every 25 °C from room temperature to 700 °C) and (b) a H_2 atmosphere (a diffractogram was recorded every 20 °C from room temperature to 620 °C).

Bi in the V site, slightly modified the final reduced compound.

(b) BITAVOX.15. In the case of BITAVOX.15, only a smooth evolution of the diffractograms is observed. BITAVOX.15 is a γ-type BIMEVOX, and its structure can be described using the tetragonal $a = 3.9$ and $c = 15.6$ Å unit cell parameters. During the first 2 h of experiment, a shift of the (1 1 0) reflection toward higher 2θ values is observed, corresponding to a decrease of the a parameter. In a concomitant way, an opposite shift of the (0 0 6) reflection toward smaller 2θ values occurs, accounting for an increase of the c parameter, characterizing the stacking direction of the sheets.

(2) Zirconium Chemical Reduction. The overall experiment that consists of removing oxygen from the α-$Bi_4V_2O_{11}$ compound by means of an oxygen acceptor such as the finely divided zirconium metal was conducted as follows. The orange-brown BIMEVOX powder was placed in a vacuum-sealed Pyrex tube containing another small rounded Pyrex tube hosting the suitable amount of Zr powder, so as to prevent any contact between the two solid reactants. The tube was then annealed for 3 days at 450 °C.

During this annealing step, the Zr color evolved from gray to white (ZrO_2), whereas the orange-brown BIMEVOX powder turned dark brown, implying a reduction of V^{5+} to V^{4+} according to the following reaction:

$$Bi_4V_2O_{11} + 0.17Zr \rightarrow Bi_4V_2O_{10.66} + 0.17ZrO_2 \quad (1)$$

The recovered dark material was analyzed by X-ray at room temperature (Figure 5), and the powder pattern was indexed in the orthorhombic cell (*Pnma*) of α-$Bi_6V_3O_{16}$ ($Bi_4V_2O_{10.66}$).

Attempts to prepare compounds with a larger reduction state (e.g., Zr content > 0.17) resulted in a multiphase sample (Figure 5) with, besides the main α-$Bi_6V_3O_{16}$ phase, the presence of Bi (as evidenced by the appearance of a Bragg peak at $2\theta = 27.3°$) and of undetermined secondary phases. Conversely, for lower Zr contents (< to 0.17), the XRD patterns of the resulting materials were always showing the coexistence of $Bi_4V_2O_{11}$ and $Bi_6V_3O_{16}$ phases, suggesting a biphasic oxygen removal process, in agreement with previous studies carried out using H_2 instead of Zr as the reducing agent as described above.

The as-made $Bi_6V_3O_{16}$ was then reoxidized in an air atmosphere at 400 °C. In all cases, it converted back to the initial oxidized $Bi_4V_2O_{11}$.

The reversible reduction of $Bi_4V_2O_{11}$ appears to be limited to one V^V over three, whatever the method used: chemical reduction by H_2 atom or by Zr acting as a acceptor. Attempts to reach a total V^V-V^{IV} reduction as claimed by Galy et al. systematically failed.

(3) Electrochemical Insertion of Lithium. BIMEVOX/Li cells were first cycled in a galvanostatic mode between 3 and 0.02 V at a C/5 rate (i.e., one Li^+ is inserted in 5 h). Whatever the nature/composition of the BIMEVOX studied, we always obtained charge/discharge traces of the type shown in Figure 6. They are very similar to those reported by the Spanish group.[9] The voltage−composition curve shows that $Bi_4V_2O_{11}$ reacts with a large number of lithiums per formula unit leading to capacities as high as 800 mA h/g. However,

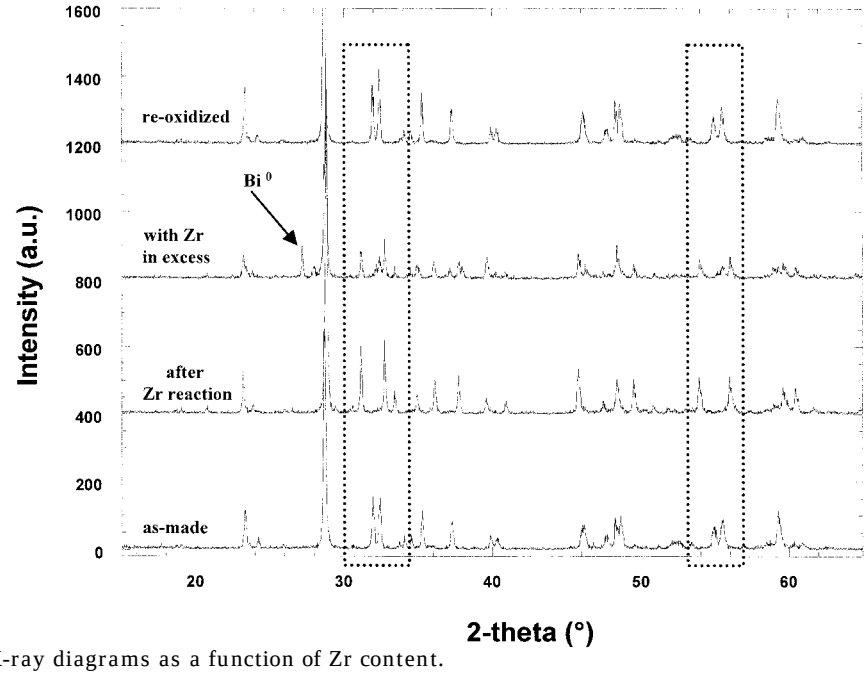

Figure 5. $Bi_4V_2O_{11}$ X-ray diagrams as a function of Zr content.

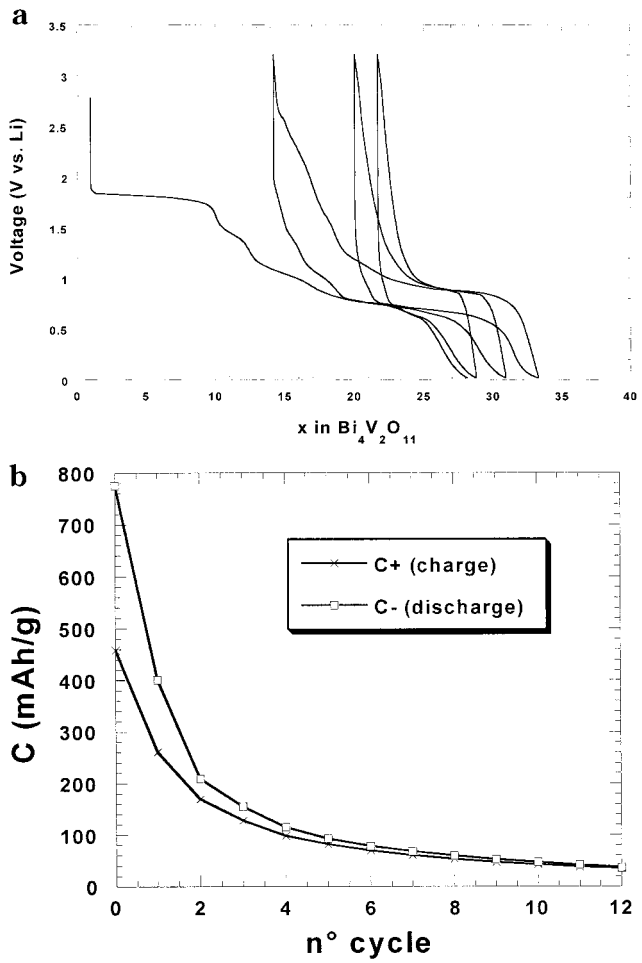

Figure 6. (a) Voltage−composition trace for a $Bi_4V_2O_{11}$/Li cell cycled between 3 and 0.02 V at a C/5 rate with (b) capacity fade of the same cell upon long cycling.

the loss in capacity between the first discharge and the first charge is quite important (about 40%). Moreover, the capacity decay as function of the cycle number reaches values as high as 50% after only a few cycles (see Figure 6b), indicating a nonreversible Li-reactivity process. Due to both the large initial irreversibility and the rapid capacity decay, these materials could by no means be used as the negative electrode for the Li-ion technology as previously claimed.[13]

To understand how the electrochemical lithium reactivity in these materials proceeds, in situ X-ray diffraction measurements on various BIMEVOX/Li electrochemical cells were pursued. The collected X-ray powder patterns for $Bi_4V_2O_{11}$ as a function of the number of reacted lithium (x) is shown in Figure 7a. The three Bragg peaks at $2\theta \approx 41$, 51, and 53°, referred to by an asterisk on the diffractograms, are due to the beryllium window. Within such experiments, XRD patterns are taken every 3 h; however, only a few of them are shown to convey the message. The Li-driven structural changes are subtle but can be nicely visualized over the 2θ ranges delimited by the dashed rectangles. As the electrochemical reduction proceeds, the two sets of double peaks, located around $2\theta = 32°$ and 55° and corresponding to the initial phase, progressively vanish while a new phase, as indicated by two other sets of more spread double peaks, grows to become predominant and unique for $x = 2$. The $x = 2$ phase that we note for commodity "$Li_2Bi_4V_2O_{11}$" has an X-ray powder pattern identical to the $Bi_6V_3O_{16}$ phase previously observed by chemical reduction. Further pursuing the lithium electrochemical reduction resulted in a progressive disappearance of the Bragg peaks corresponding to $Li_2Bi_4V_2O_{11}$ together with the appearance of a few weak Bragg peaks (the most intense one being located at $2\theta \approx 27°$), and finally to a featureless X-ray powder pattern (reminiscent of an amorphous material) when the Li content exceeded 28 lithiums per formula unit. Upon subsequent charge/discharge cycles, the material remained amorphous.

Interestingly, by recharging the partially reduced $Li_2Bi_4V_2O_{11}$/Li cell (e.g., oxidation) the reduced phase does not convert back to the starting material.

(13) Arroyo y de Dompablo, M. E.; Moran, E.; Garcia-Alvarado, F. *J. Inorg. Mater.* **1999**, *1*, 83.

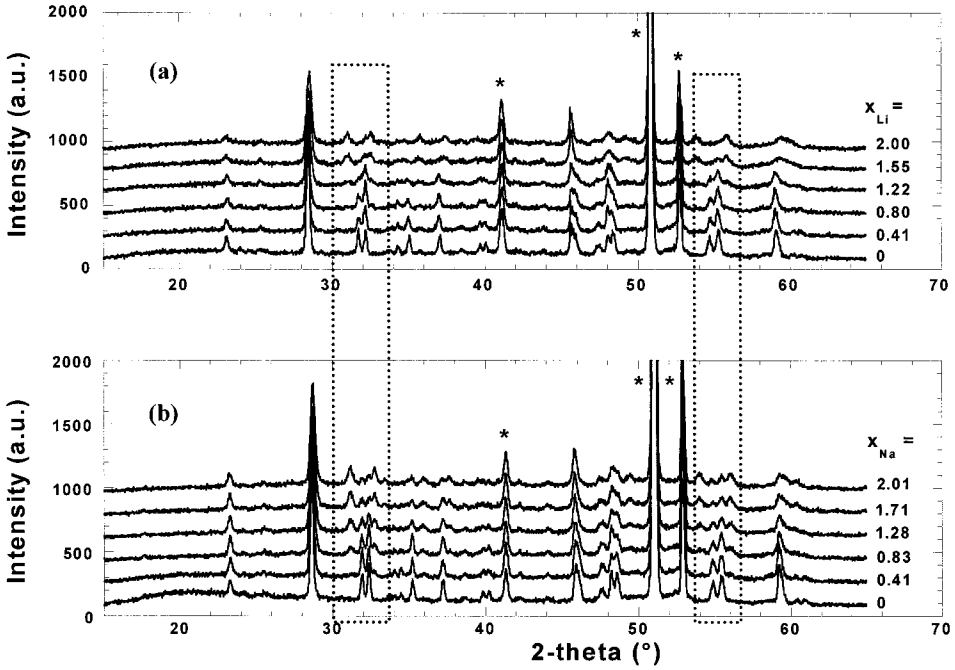

Figure 7. in Situ X-ray powder diffractograms collected at various states of discharge (up to $x = 2$) of (a) $Bi_4V_2O_{11}$/Li and (b) $Bi_4V_2O_{11}$/Na cells. The dotted outlined rectangles highlight the two domains over which Li/Na driven Bragg peak changes are the most prominent. The asterisks denote the Bragg peaks corresponding to the Be window.

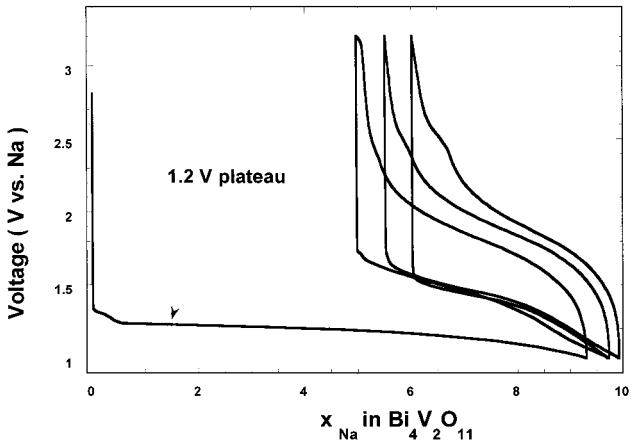

Figure 8. Voltage−composition trace for a $Bi_4V_2O_{11}$/Na cell using a solution of 1 M $NaClO_4$ in propylene carbonate as the electrolyte, cycled between 3 and 1.1 V at a C/5 rate.

These results question the role played by lithium during the reduction process. Are we dealing with a classical insertion/deinsertion process or a Li-driven decomposition process leading to the formation of Li_2O?

In the former case, one would expect the amount of ions inserted into the BIMEVOX host structure to be dependent on their ionic radii. To test the radii effect, an in situ X-ray $Bi_4V_2O_{11}$/Na cell ($r_{Li}^+ = 0.60$ Å, $r_{Na}^+ = 0.95$ Å) was assembled and XRD powder patterns were collected while the cell was discharged. Figure 8 shows the voltage composition trace for such a cell, which presents a plateau of capacity amplitude similar to the one observed for the lithium cell with the difference that it occurs at lower potential (1.2 for Na instead of 1.8 for Li). The sodium electrochemical reduction induces structural changes similar to those previously noted for Li, which can be visualized over the same 2θ ranges (Figure 7b). Indeed, as the sodium reduction proceeds beyond $x = 0.8$, we note, besides the main Bragg peaks, the appearance of a few extra peaks corresponding to $Bi_6V_3O_{16}$, indicating a biphasic process. Therefore, a difference between the Li and Na reduction process resides in the extent of the biphasic process that is under $x = 2$ for Li while it extends beyond $x = 2$ for Na. For the latter, upon further Na reduction, a complete amorphization of the electrode material was reached prior to noticing any evidence for the existence of single-phase "$Na_xBi_6V_3O_{16}$" material. This observation further supports an alkali-driven electrochemical oxygen removal process.

In situ X-ray powder patterns corresponding to BIBIVOX.02 and BITAVOX.15 used as positive electrode, discharged down to 0.02V at the C/50 rate, are reported in Figure 9. The transformation is, as for reduction process, softer than for the parent compound. In the case of BIBIVOX, for $x = 1.97$, the characteristic peaks of $Bi_6V_3O_{16}$ just begin to appear. In the case of BITAVOX.15, a tiny shift in the peak position and the appearance of an extra peak at 27° in 2θ, corresponding to Bi metal, are to be noticed from $x = 0.23$. For x values larger than 0.53−1.50, the diagrams remain the same. This evolution is in total accordance with the behavior of this phase under reductive atmosphere (except the extra peak corresponding to Bi metal, not visible at 350 °C since the bismuth melting point is 271.3 °C) and confirm the material reduction during the electrochemical process.

Moreover, as $Bi_4V_2O_{11}$, these materials underwent a transition into an amorphous phase as soon as the reduction was extended beyond the 1.8 V plateau.

To obtain better insight into the origin of the different Li-induced structural behavior between the $Bi_4V_2O_{11}$ and BIBIVOX compounds for amounts of reacted lithium lower than 2, we decided to use electrochemistry as a spectroscopy technique. The first discharges of batteries using $Bi_4V_2O_{11}$ and BIBIVOX ($Bi_2V_{1-x}Bi_xO_{5.5-\delta}$, where $x = 0.02$, 0.04, and 0.06) were studied at a low current

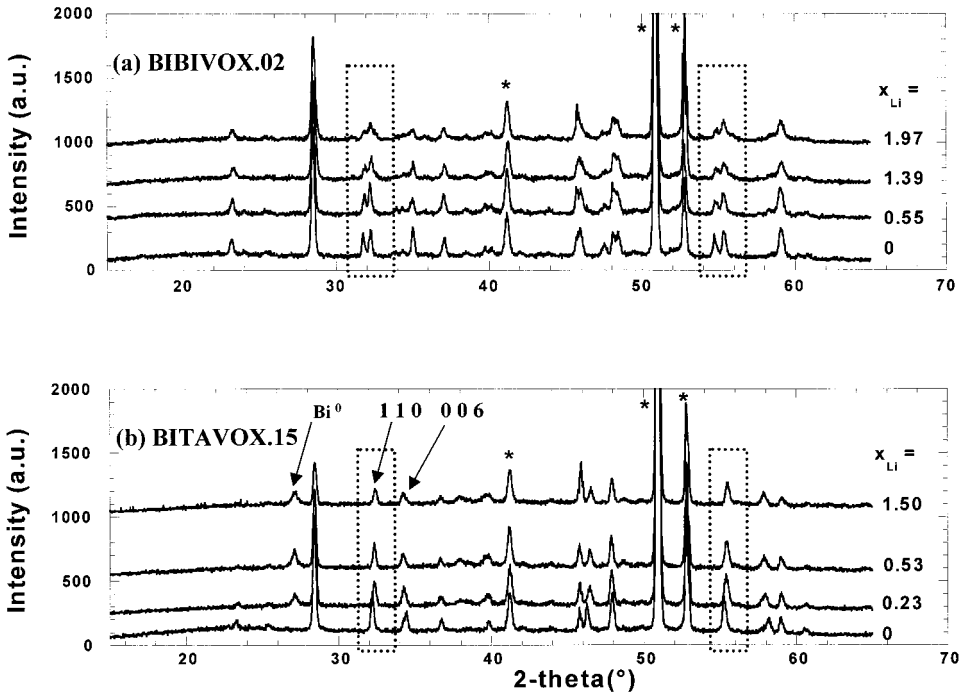

Figure 9. in Situ X-ray powder diffractograms collected at various states of discharge of (a) BIBIVOX/Li and (b) BITAVOX/Li cells. The dotted outlined rectangles highlight the two domains over which most of the changes were expected according to Figure 7. The asterisks denote the Bragg peaks corresponding to the Be window.

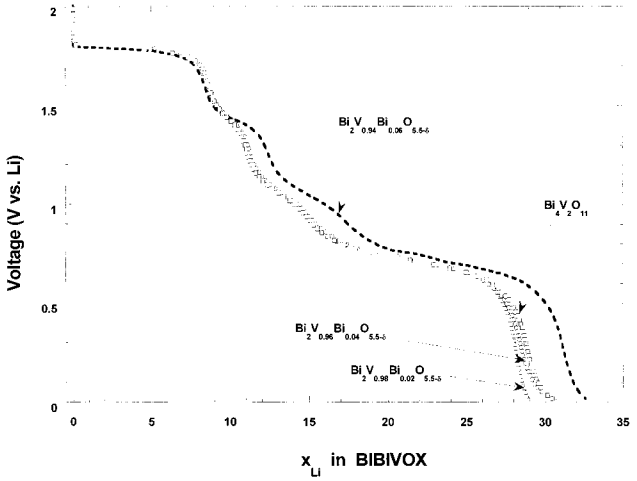

Figure 10. Voltage−composition curves for various BIMEVOX/Li cells using members of the BIBIVOX series (x = 0, 0.02, 0.04, 0.06) as positive electrodes, discharged at the same current rate of C/100.

rate (C/100) in a galvanostatic mode. The voltage−composition traces perfectly superimposed, with the exception of the $x = 0.06$ BIBIVOX phase (Figure 10). However, caution has to be exercised prior to interpreting this difference, since $x = 0.06$ is the upper Bi limit for the existence of the BIBIVOX solid solution range;[14] therefore, the compound may not be phase pure. For a better comparison, we drew (but do not show) the derivative curves dx/dV. This mathematical tool, equivalent to a potentiostatic mode, shows the same potential value whether the samples are Bi- or non-Bi-substituted, preventing then any satisfactory conclusion as to the origin of the observed Li-driven structural differences, with the exception that the Li reactivity mechanism in these materials is different from the classical Li insertion/deinsertion mechanism as will be further discussed.

Discussion

When using metallic zirconium, the oxygen-deficient single-phase $Bi_6V_3O_{16}$ material was obtained when the right amount of Zr (0.17) was reacted at temperatures ranging from 400 to 500 °C to remove 0.33 oxygen atoms (ZrO_2). Similarly, it was reported that over the same temperature range H_2 reacted with 0.33 oxygen from the $Bi_4V_2O_{11}$ to produce the reduced $Bi_6V_3O_{16}$ ($Bi_4V_2O_{10.66}$) phase. During these reduction reactions, as oxygen was removed from the precursor phase, 0.33 V^V cations were reduced to V^{IV}. In both cases, further reduction by adding excess of Zr or enhancing the H_2 reacting time or temperature led to decomposition products.

When dealing with the reactivity of Li toward inorganic compounds, one can have either insertion-type or decomposition reactions. For a lithium insertion to occur, the host material (herein $Bi_4V_2O_{11}$) must have, among others, an open framework structure containing empty crystallographic sites to accept lithium ions, and must contain redox centers. From the Zr or H_2 reducing experiments, we know that vanadium cations provide the latter condition. In contrast, from the existing structural data, the existence of interstitial sites for Li within the $Bi_4V_2O_{11}$ framework structure is more questionable.

Another main characteristic of Li insertion reactions is their reversibility. Thus, our inability to electrochemically recharge our $Li_2Bi_4V_2O_{11}$ material strongly suggests that we are dealing with a decomposition reaction rather than an insertion/deinsertion reaction. Therefore, we note that our material referred to as $Li_2Bi_4V_2O_{11}$ all along has an X-ray powder pattern similar to that of $Bi_6V_3O_{16}$. Thus, one believes that once the electrochemi-

(14) Vannier, R. N.; Mairesse, G.; Abraham, F.; Nowogrocki, G. *Solid State Ionics* **1994**, *70/71*, 248.

cal reduction of $Bi_4V_2O_{11}$ proceeds, the following reaction leading to the formation of amorphous Li_2O and of the oxygen deficient phase proceeds:

$$Bi_4V_2O_{11} + x\ Li^+ + xe^- \rightarrow Bi_4V_2O_{11-x/2} + (x/2)Li_2O \quad (2)$$

According to eq 2, 0.66 lithium is needed to remove 0.33 oxygen. From X-ray data, we note that the $Bi_4V_2O_{10.66}$ ($Bi_6V_3O_{16}$) phase appears near $x = 1.5$, but 2 lithiums are needed to obtain the material as single phase. Meanwhile to account for the reduction of $Bi_4V_2O_{11}$ with sodium it required only 0.8 Na^+. Presently, we do not have a coherent explanation to account for the difference between the expected amount of lithium for eq 2 and the experimental values with the exception of secondary electrochemical reactions leading to either (1) the formation of a solid electrolyte interface (SEI) containing lithium or (2) the formation of amorphous products. However, the fact that the reactivity of these materials toward Li and Na proceeds similarly (phase changes occur for the same x) while these cations are of different sizes is another indirect proof in favor of a decomposition process since the number of ions (x) inserted into a structure depends on the size of the guest cation. Such a type of decomposition reaction is not unusual when studying the Li reactivity on oxide compounds not having an open-framework type structure for Li insertion. Indeed, SnO_2, a material of choice for the anode in Li-ion battery, was for instance shown to decompose at the early stage of the reduction process into Li_2O and Sn, the latter reversibly alloying with lithium and the former playing the role of an inert electrochemical medium.[15]

Now, let us go back to the large amount of reacted lithium that can reach values as high as 32 lithium ions per $Bi_4V_2O_{11}$ unit formula, with the end material being amorphous $Li_{32}Bi_4V_2O_{11}$ as deduced by X-ray. On the basis of the classical Li insertion/deinsertion mechanism, even by assuming a complete reduction of all the cations (i.e., $2V^V \rightarrow 2V^0$ and $4Bi^{III} \rightarrow 4Bi^0$), the expected amount of inserted Li ions should be limited to 22 per unit formula. Thus, only a Li-driven decomposition reaction can account for the observed large amount of reacted lithium. Unfortunately, such a large initial capacity rapidly decays upon subsequent cycles. Neither the large initial capacity uptake nor the decay upon cycling are specific to the BIMEVOX-type compounds. Interestingly, by compiling the work presently done on numerous oxide negative electrodes (SnO_2[16] and vanadates),[17] they all tend to show a large initial capacity, amorphization during the first discharge with the formation of nanoparticles, and a rapid capacity decay. For the vanadates (M−V−O) that do not contain a metal cation alloying with lithium, we proposed, to account for the large amount of reacted lithium, a model consisting of the Li adsorption−desorption on electrochemically made nanoparticles involving the formation of "Li-O" bonds. In light of this general trend, the Li reactivity mechanism is most likely of the same type with, in addition, the possibility of Li alloying with Bi (Li_xBi). Thus, for Li amounts greater than 2, $Bi_6V_3O_{16}$ will react with lithium as follows:

$$Bi_6V_3O_{16} + yLi^+ + ye^- \rightarrow \text{amorphous material}$$
$$(y-x-zLi_2O + Li_xBi + x-y+2zV-O-Li) \quad (3)$$

with the Li_2O of eqs 2 and 3 being responsible for the large (40%) irreversibility between the first discharge and charge, and with the origin of the rapid capacity decay being nested in the alloy's particle agglomeration upon cycling as well as on the enhanced electrolyte reduction on highly divided materials. Further experimental work, namely, XANES and EXAFS measurements and extended in situ X-rays upon cycling, is presently in progress to test the above proposed BIMEVOX reactivity mechanism toward lithium.

Acknowledgment. The authors are grateful to J-B. Leriche and M. Nelson for their technical assistance.

CM001149C

(15) Mao, O.; Dahn, J. R. *J. Electrochem. Soc.* **1999**, *146*, 414; 423.

(16) Courtney, I. A.; McKinnon, W. R.; Dahn, J. R. *J. Electrochem. Soc.* **1999**, *146*, 59.

(17) Denis, S.; Baudrin, E.; Orsini, F.; Ouvrard, G.; Touboul, M.; Tarascon, J.-M. *J. Power Sources* **1999**, *79*, 81.